Strain-Induced Polarization Rotation in Epitaxial (001) $BiFeO_3$ Thin Films

H. W. Jang,[1] S. H. Baek,[1] D. Ortiz,[1] C. M. Folkman,[1] R. R. Das,[1] Y. H. Chu,[2] P. Shafer,[2] J. X. Zhang,[3] S. Choudhury,[3]
V. Vaithyanathan,[3] Y. B. Chen,[4] D. A. Felker,[5] M. D. Biegalski,[6] M. S. Rzchowski,[5] X. Q. Pan,[4] D. G. Schlom,[7]
L. Q. Chen,[3] R. Ramesh,[2] and C. B. Eom[1,*]

[1]*Department of Materials Science and Engineering, University of Wisconsin, Madison, Wisconsin 53706, USA*
[2]*Department of Physics and Department of Materials Science and Engineering, University of California, Berkeley, California 94720, USA*
[3]*Department of Materials Science and Engineering, Pennsylvania State University, Pennsylvania, 16802-5005, USA*
[4]*Department of Materials Science and Engineering, University of Michigan, Ann Arbor, Michigan 48109, USA*
[5]*Department of Physics, University of Wisconsin, Madison, Wisconsin 53706, USA*
[6]*Center for Nanophase Materials Sciences, Oak Ridge National Laboratory, Oak Ridge, Tennessee 37831, USA*
[7]*Department of Materials Science and Engineering, Cornell University, Ithaca, New York, 14853-1501, USA*

(Received 21 February 2008; published 4 September 2008)

Direct measurement of the remanent polarization of high quality (001)-oriented epitaxial $BiFeO_3$ thin films shows a strong strain dependence, even larger than conventional (001)-oriented $PbTiO_3$ films. Thermodynamic analysis reveals that a strain-induced polarization rotation mechanism is responsible for the large change in the out-of-plane polarization of (001) $BiFeO_3$ with biaxial strain while the spontaneous polarization itself remains almost constant.

DOI: 10.1103/PhysRevLett.101.107602 PACS numbers: 77.84.Dy, 77.22.Ej, 77.55.+f, 77.65.−j

The strong coupling between polarization and strain in ferroelectrics allows the control of properties by strain, namely, strain engineering [1]. Indeed, drastic strain-induced enhancements in ferroelectric Curie temperatures and polarization have been observed in a number of epitaxial complex oxide thin films [2,3]. However, a recent first-principles study on $BiFeO_3$ shows a significantly different behavior; the polarization of a $(111)_p$-oriented $BiFeO_3$ film (where the subscript p denotes pseudocubic indices) is almost independent of strain [4,5].

In this Letter, we study the strain dependence of the remanent polarization of $BiFeO_3$ through direct measurements on the *same* epitaxial $(001)_p$ $BiFeO_3$ thin-film capacitors before and after releasing them from an underlying Si substrate to which they were strained and clamped. Our measurements reveal that the out-of-plane polarization (P_3) of $(001)_p$-oriented $BiFeO_3$ thin films has a strong strain dependence, even stronger than (001)-oriented $PbTiO_3$ films [6]. This is in direct contrast to $(111)_p$-oriented $BiFeO_3$ which, according to first-principles calculations, shows very little strain dependence of P_s [4,5]. The objective of this study is to understand the physical origin for the strong orientation-dependence of strain tunability of $(001)_p$-oriented $BiFeO_3$ thin films.

Bulk $BiFeO_3$ has a rhombohedrally distorted perovskite structure with unit cell parameters $a = 5.6343$ Å and $\alpha_r = 59.348°$ [7]. It possesses a large intrinsic spontaneous polarization (P_s) $\sim 100\ \mu C/cm^2$ along the [111] direction at room temperature [8,9]. In the case of thin films, owing to mismatch in lattice parameters or thermal expansion between the films and the underlying substrates, large strains can be generated—well beyond where they would fracture in bulk form—resulting in material properties significantly different from those obtained for the bulk structures [1–3]. Epitaxial $(001)_p$ $BiFeO_3$ films grown on (001) $SrTiO_3$ substrates are subjected to a *compressive* strain due to the lattice mismatch of −1.4%. In contrast, epitaxial $(001)_p$ $BiFeO_3$ films grown on (001) Si substrates are under biaxial *tensile* strain due to the difference in thermal expansion between the film and the substrate.

Since the amount of strain resulted from lattice mismatch decreases with the thickness of the $BiFeO_3$ films due to strain relaxation, different states of compressive and tensile strains can be obtained by changing the thickness of the $BiFeO_3$ films. Thus, we have examined the strain dependence of the ferroelectric properties of $BiFeO_3$ using compressively strained films on (001) $SrTiO_3$ substrates, tensilely strained films on (001) Si substrates, and strain-free membranes after lift-off. The procedure used to lift off the $BiFeO_3$ film, while preserving its measurement electrode, is described elsewhere [10]. We measured exactly the same capacitors before and after the removal of the substrates, which excludes all other extrinsic variables that affect the ferroelectric properties of $BiFeO_3$.

The epitaxial arrangement and crystalline quality of $BiFeO_3$ thin films and strain-free membranes were studied by high resolution four-circle x-ray diffraction (HRXRD) and transmission electron microscopy (TEM). Figure 1(a) shows a cross sectional TEM image of a $BiFeO_3/SrRuO_3/SrTiO_3$ heterostructure grown on a 4°-miscut (001) Si substrate by off-axis sputtering [11]. Fringes parallel to the $[101]_p$ direction in the $BiFeO_3$ thin film are 71° ferroelectric domain walls, confirmed by both the high resolution lattice imaging and the selected area electron diffraction. The full width at half maximum (FWHM) of the rocking curve of 002_p $BiFeO_3$ for $BiFeO_3$ films on miscut (001) Si substrates was very similar to that for $BiFeO_3$ films grown on miscut (001) $SrTiO_3$ substrates,

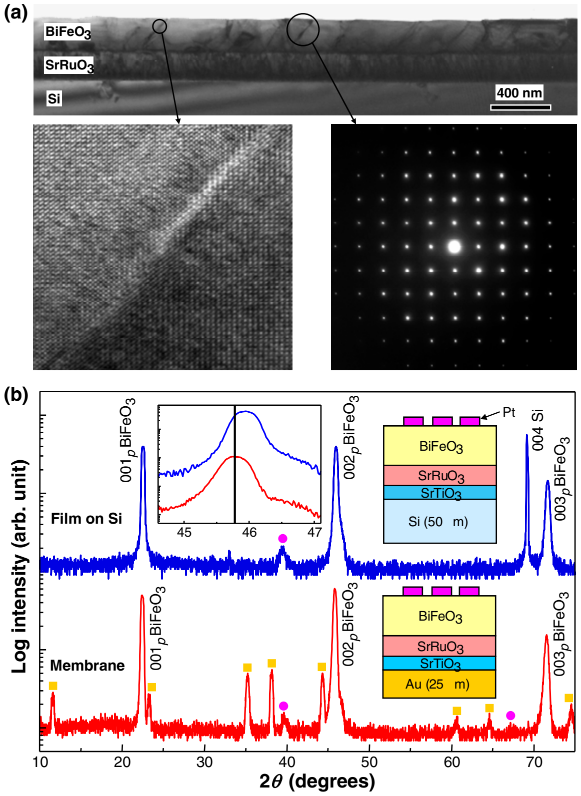

FIG. 1 (color online). (a) Typical bright-field TEM image of a $BiFeO_3/SrRuO_3/SrTiO_3$ heterostructure grown on a 4°-miscut (001) Si substrate showing 71° ferroelectric domains along the $[101]_p$ direction. A high resolution TEM image of $BiFeO_3$ at a 71° ferroelectric domain wall in the $BiFeO_3$ film and an electron diffraction pattern from the indicated $BiFeO_3$ region are shown. (b) HRXRD $\theta - 2\theta$ scans of 400-nm-thick $BiFeO_3$ films before and after lift-off, ● and ■ correspond to diffraction peaks from Pt top electrodes and the Au plate, respectively. The insets show an expanded view around the 002_p $BiFeO_3$ peaks with the vertical line for the 2θ value of bulk 002_p $BiFeO_3$.

indicating that the crystalline quality of $BiFeO_3$ film on (001) Si is as good as those grown on single crystal (001) $SrTiO_3$ substrates. Figure 1(b) shows x-ray diffraction $\theta - 2\theta$ scans of a 400-nm-thick as-grown $BiFeO_3$ film on (001) Si and a $BiFeO_3$ membrane after lift-off. The diffraction pattern of the as-grown film reveals that it is single-phase and $(001)_p$ oriented. For the $BiFeO_3$ membrane, the 004 Si peak disappears and diffraction peaks from the Au counter electrode deposited during the lift-off process [10] are observed. The systematic shift of the $00l$ peaks towards lower diffraction angles after lift-off indicates an increase in the out-of-plane lattice parameter of the film. The out-of-plane lattice parameter of the as-grown film was found to be 3.943 Å, which is smaller than that of bulk $BiFeO_3$, 3.96 Å. This indicates that the as-grown film is subjected to a biaxial *tensile* strain in the plane of the film due to the large mismatch of thermal expansion coefficients between the Si substrate and $BiFeO_3$ film. As can be seen in the inset of Fig. 1(b), the out-of-plane lattice parameter of the membrane is the same as that of bulk $BiFeO_3$, suggesting that the as-grown film is subjected to an elastic strain which is fully relieved after lift-off.

HRXRD reciprocal space maps (RSMs) of the $BiFeO_3$ films were made before and after lift-off to determine the crystal symmetry and 3-dimensional strain state. Figure 2(a) shows RSMs of the as-grown 400-nm-thick $BiFeO_3$ film around the 113_p reflection. The obtained RSMs show two peaks as a consequence of the existence of two domains. The RSMs for the $BiFeO_3$ membrane in Fig. 2(b) also show peak splitting into two domains, supporting the idea that the overall domain structure was maintained after the lift-off process. The diagonal peak shape seen for the membrane indicates that strain relief led to an increase of the mosaic spread of the film along the $(101)_p$ domain walls. Analysis of the RSMs of the as-grown film reveals that there is no change in the peak splitting along the $[00l]_p$ direction following an azimuthal rotation by 180°, whereas the membrane shows two different peak splitting with such an azimuthal rotation. In the RSM, peak splitting along the $[00l]_p$ direction means that there are planes with different d-spacings [12]. Thus, the as-grown film is found to possess two different d-spacings for the 113_p reflection, but the membrane contains three different d-spacings. Taking this into consideration, the

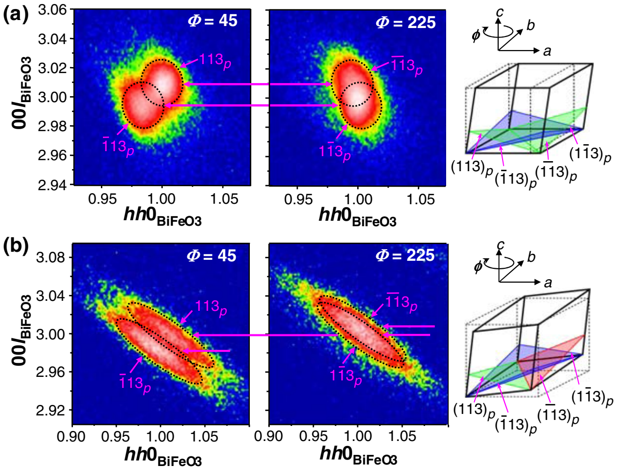

FIG. 2 (color online). (a) Reciprocal-space maps of the 400-nm-thick as-grown film on a Si substrate. Reciprocal-space images of the 113_p reflection show two peaks (domains) marked with a dotted line. After rotating the film azimuthally by 180°, the peak splitting along the $[00L]_p$ direction was unchanged. This is because the as-grown film has monoclinic symmetry, in which the 113_p reflection has twofold symmetry with two different d-spacings shown in the schematic drawing of the $\{113\}_p$ planes in the unit cell. (b) Reciprocal-space maps of the strain-free $BiFeO_3$ membrane. After rotating the film azimuthally by 180°, the image shows different peak splitting along the $[00L]_p$ direction. This is because the membrane has rhombohedral symmetry, in which the 113_p reflection does not have twofold symmetry and there are three different d-spacings as shown in the schematic drawing of the $\{113\}_p$ planes in the unit cell.

HRXRD RSM results confirm that the crystal structure of the $BiFeO_3$ membrane is rhombohedral, while that of the as-grown film is monoclinic.

The unit cell dimensions of the 400-nm and 600-nm-thick as-grown $BiFeO_3$ films on (001) Si were determined to be $a = 3.965$ Å, $b = 3.990$ Å, $c = 3.946$ Å, $\beta = 89.52°$ and $a = 3.967$, $b = 3.996$, $c = 3.943$, and $\beta = 89.51°$, respectively. In contrast, the 400-nm and 600-nm-thick $BiFeO_3$ membranes were both found to have a rhombohedral unit cell with $a = b = c = 3.960$ Å and $\alpha = 89.4°$, which is the same as that of bulk $BiFeO_3$ single crystals.

To investigate the effect of both strain relaxation and crystal symmetry on the ferroelectric properties of $BiFeO_3$ films, polarization-electric field (P-E) hysteresis loop measurements were carried out on both 400 nm and 600 nm thick $BiFeO_3$ films before and after lift-off using a Precision Fast Hysteresis 100 V ferroelectric tester from Radiant Technologies, Inc. Figure 3 shows the P-E hysteresis loops measured at a frequency of 20 kHz for the 400-nm-thick $BiFeO_3$ film before and after lift-off. The strain-free membrane shows appreciably larger polarization values than the as-grown sample. After measuring the *same* five circular dots each with 100 μm diameter before and after lift-off, the remanent polarization (P_r) was determined to be $52 \pm 2\ \mu C/cm^2$ for the as-grown film, and $58 \pm 1\ \mu C/cm^2$ for the strain-free membrane, respectively. Comparison with the P-E hysteresis loop of the 400-nm-thick $BiFeO_3$ film on the $SrTiO_3$ substrate leads to the finding that the P_r value of the strain-free membrane is between those of the *tensile*-strained film on (001) Si and *compressively* strained film on (001) $SrTiO_3$ ($64 \pm 2\ \mu C/cm^2$). The same result was also found for the 600-nm-thick $BiFeO_3$ film and membrane, confirming the change of P_r with biaxial strain.

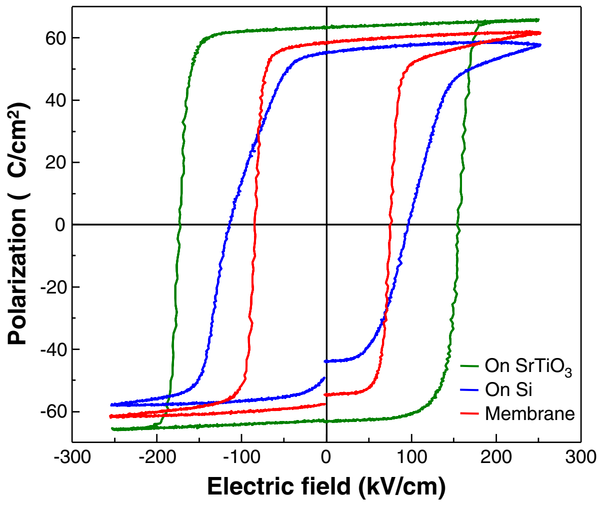

FIG. 3 (color online). Polarization-electric field (P-E) hysteresis loops of a 400-nm-thick as-grown $BiFeO_3$ film grown on Si and a strain-free $BiFeO_3$ membrane. Both loops were obtained from the same capacitor before and after lift-off. The P-E hysteresis loop of a 400-nm-thick $BiFeO_3$ film grown on a $SrTiO_3$ substrate is shown for comparison. The membrane exhibits a significantly reduced coercive field. The discontinuity at zero electric field (negative polarization axis) for $BiFeO_3$ membranes and $BiFeO_3$ on Si is due to a strong built-in bias in the films.

The projection of the measured P_r of the strain-free membrane onto the $[111]_p$ $BiFeO_3$ direction leads to a value of $\sim 101\ \mu C/cm^2$. Recently, we obtained a polarization value of $102 \pm 2\ \mu C/cm^2$ from fully relaxed $(111)_p$-oriented $BiFeO_3$ films grown on a (111) $SrTiO_3$ substrate [10]. These results convincingly established the intrinsic nature of the large spontaneous polarization of $BiFeO_3$.

To clarify the strain dependence of the remanent polarization of $BiFeO_3$, the P_r values of $(001)_p$ $BiFeO_3$ films on (001) $SrTiO_3$ and Si substrates and membrane samples were plotted as a function of in-plane strain in Fig. 4(a). The biaxial in-plane strains of films and membranes were determined from in-plane lattice parameters measured by HRXRD-RSM. Figure 4(a) shows an approximately linear relationship between the remanent polarization of $BiFeO_3$ and the in-plane strain. Our experimental data on $(001)_p$-oriented $BiFeO_3$ films exhibit a ~25% change in P_r for a 1.0% in-plane strain, higher than the 16% change in P_r for $PbTiO_3$ [13,14] and comparable to the 33% change in P_r for $BaTiO_3$ [15] for the same amount of in-plane strain, and in stark contrast to the strain dependence of P_r $(111)_p$-oriented $BiFeO_3$ films (~1.3% change in P_s for a 1.0% in-plane strain) [5]. From measurements of P-E hysteresis loops of $BiFeO_3$ films on $SrTiO_3$ and Si substrates from room temperature to 8 K, we found that there is no temperature dependence of P_r values for $(001)_p$ $BiFeO_3$ films, which indicates that the strong strain dependence of P_r in $(001)_p$ $BiFeO_3$ is valid over a wide temperature range.

In order to understand the strain dependence of the polarization of $BiFeO_3$ films, we performed a thermodynamic analysis [16]. As expected, the in-plane components of polarization (P_1 and P_2) are not equal to the out-of-plane component (P_3) due to the substrate constraint; compressive substrate strains lead to an increase in P_3 and a decrease in P_1 and P_2, while tensile substrate strains have the opposite effect. As a result, the symmetry of the $BiFeO_3$ film becomes monoclinic, labeled as the M_A phase for compressive strain and the M_B phase for tensile strain, respectively, as shown in Fig. 4(b). The predicted strain dependence of the out-of-plane polarization (P_3) shows excellent agreement with the experimental data (P_r). It is remarkable, however, that the absolute magnitude of the spontaneous polarization ($P_s = |\boldsymbol{P}|$) is almost independent of in-plane substrate strain as shown by the green triangles in Fig. 4(a); i.e., the polarization of a $(001)_p$ $BiFeO_3$ film simply rotates from the $[111]_p$ direction towards the $[001]_p$ direction under compressive biaxial strain and towards the $[110]_p$ direction for tensile strain, without appreciable change in its magnitude. It should be noted that

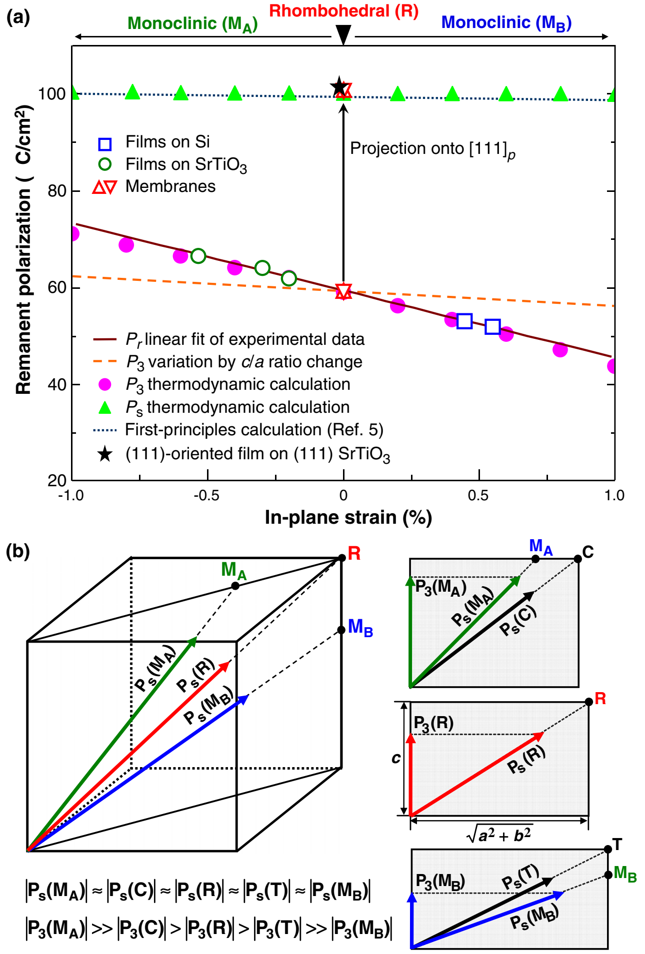

FIG. 4 (color online). (a) Remanent polarization as a function of the in-plane strain of $(001)_p$ $BiFeO_3$ films grown on $SrTiO_3$ and Si substrates and strain-free $(001)_p$ $BiFeO_3$ membranes. The experimental data are very consistent with the P_3 values obtained from thermodynamic calculations, (b) The spontaneous polarization directions of the rhombohedral (R) and monoclinic (M_A and M_B) phases of $BiFeO_3$. The monoclinic M_A and M_B phases occur for biaxial compressive and tensile strains, respectively. In-plane strains induce the rotation of the spontaneous polarization in the $(110)_p$ plane. For M_A and M_B phases, the rotation of P_s is much more pronounced than the simple rotation of P_s by the change in the c/a ratio (denoted by C and T).

the rotation of P_s for the M_A and M_B phases is much larger than the simple rotation of P_s due to the different c/a ratios of the C and T phases in Fig. 4(b). The rotation due strictly to a change in the c/a ratio corresponds to only an ~5% change in P_3 for a 1.0% in-plane strain [4,17], as plotted in Fig. 4(a). The strain dependence of the spontaneous polarization of a $(001)_p$-oriented rhombohedral crystal is linearly proportional to $Q_{11} + 2Q_{12}$, where Q_{11} and Q_{12} are electrostrictive coefficients in Voigt notation. The value of $Q_{11} + 2Q_{12}$ is very small for $BiFeO_3$ [16], leading to the rotation of P_s by the in-plane strain. Such a polarization rotation has been reported in rhombohedral $Pb(Mg_{1/3}Nb_{2/3})O_3$-$PbTiO_3$ (PMN-PT) bulk single crystals [18,19]. Our finding, however, differs from the previous work in that the polarization rotation in $BiFeO_3$ films is induced by in-plane strain, whereas that in PMN-PT is induced by an external electric field.

We also computed the spontaneous polarization of a $(111)_p$-oriented $BiFeO_3$ film as a function of strain using thermodynamic analysis with the same set of coefficients as for the $(001)_p$-oriented films. In agreement with earlier first-principles calculations [4,5], the strain-tunability of $(111)_p$-oriented $BiFeO_3$ is much smaller than that of $(001)_p$-oriented tetragonal $PbTiO_3$ and $BaTiO_3$ films, indicating that the magnitude of the spontaneous polarization is insensitive to strain for $BiFeO_3$. This is consistent with the fact that the spontaneous polarization rotates in response to biaxial strain in $(001)_p$ $BiFeO_3$ films rather than changing its magnitude.

In conclusion, we have provided direct experimental evidence that $(001)_p$-oriented $BiFeO_3$ films exhibit a strong strain tunability of their out-of-plane remanent polarization. It is shown that this strain tunability results from a strain-induced rotation mechanism of the spontaneous polarization direction.

The authors gratefully acknowledge the financial support of the National Science Foundation through Grants Nos. ECCS-0708759, DMR-0507146, and DMR-0820404; the Office of Naval Research through Grants Nos. N00014-07-1-0215 and N00014-04-1-0426; and the Department of Energy under Grant No. DE-FG02-07ER46417. We also acknowledge the support of the Division of Scientific User Facilities, Basic Energy Sciences, US DOE.

---

*eom@engr.wisc.edu

[1] D. G. Schlom *et al.*, Annu. Rev. Mater. Res. **37**, 589 (2007).
[2] J. H. Haeni *et al.*, Nature (London) **430**, 758 (2004).
[3] K. J. Choi *et al.*, Science **306**, 1005 (2004).
[4] C. Ederer and N. A. Spaldin, Phys. Rev. B **71**, 224103 (2005).
[5] C. Ederer and N. A. Spaldin, Phys. Rev. Lett. **95**, 257601 (2005).
[6] J. X. Zhang *et al.* (unpublished).
[7] F. Kubel and H. Schmid, Acta Crystallogr. Sect. B **46**, 698 (1990).
[8] J. B. Neaton *et al.*, Phys. Rev. B **71**, 014113 (2005).
[9] P. Ravindran *et al.*, Phys. Rev. B **74**, 224412 (2006).
[10] H. W. Jang *et al.*, Appl. Phys. Lett. **92**, 062910 (2008).
[11] R. R. Das *et al.*, Appl. Phys. Lett. **88**, 242904 (2006).
[12] J. F. Li *et al.*, Appl. Phys. Lett. **84**, 5261 (2004).
[13] C. Lichtensteiger *et al.*, Phys. Rev. Lett. **94**, 047603 (2005).
[14] D. D. Fong *et al.*, Phys. Rev. B **71**, 144112 (2005).
[15] J. B. Neaton, C. L. Hsueh, and K. M. Rabe, arXiv:cond-mat/0204511.
[16] J. X. Zhang *et al.*, J. Appl. Phys. **101**, 114105 (2007).
[17] D. H. Kim *et al.*, Appl. Phys. Lett. **92**, 012911 (2008).
[18] H. Fu and R. E. Cohen, Nature (London) **403**, 281 (2000).
[19] B. Noheda *et al.*, Phys. Rev. Lett. **86**, 3891 (2001).